MEASUREMENT OF MECHANICAL VIBRATION OF SRILAC CAVITIES

O. Kamigaito*, K. Ozeki, N. Sakamoto, K. Suda, K. Yamada,
RIKEN Nishina Center for Accelerator-Based Science, Wako-shi, Saitama, Japan

Abstract

Mechanical vibration of quarter-wavelength resonators of SRILAC, the superconducting booster of the RIKEN heavy-ion linac, was measured during a vertical cold test. The measurements were performed for fully assembled cavities as well as for bare niobium cavities without the titanium jacket. In the procedure, the instantaneous resonant frequencies were measured for 10 seconds at a time interval of 1 ms and were recorded as a time series. The frequencies were analyzed by means of conventional signal analysis. The power spectrum was deduced from the autocorrelation function calculated with the fluctuation of resonant frequencies. Although the vibration amplitudes were smaller in the cavities assembled with the titanium jacket, we could not find a clear reason for this.

INTRODUCTION

Since 2016, an upgrade project of RIKEN heavy ion linac, RILAC [1], has been started at RIKEN RI Beam Factory [2, 3], in order to promote the scientific research of superheavy elements as well as to enhance the production capability of short-lived radioisotopes, such as ^{211}At. The project attempts to increase the intensities and energies of metallic ion beams by the introduction of a superconducting ECR ion source [4] and a superconducting linac booster. The superconducting booster, named SRILAC (Superconducting RILAC), consists of ten quarter-wavelength resonators of 73 MHz contained in three cryomodules and is designed to have a total acceleration voltage of 18 MV. The construction status and cavity performance are reported elsewher [5–8].

The present paper reports in detail the measurement of the mechanical vibration of the SRILAC cavities carried out during the vertical cold test. The fluctuation of the resonant frequency is related to the mechanical vibration as follows [9–11]. First, the shift of the resonant frequency $\Delta\omega(t)$ can be written as the sum of the contributions $\Delta\omega_\mu(t)$ of the mechanical vibration mode μ:

$$\Delta\omega(t) = \sum_\mu \Delta\omega_\mu(t). \quad (1)$$

Second, in the cw operation, the frequency shift is written as $\Delta\omega_\mu(t) = \Delta\omega_{\mu 0} + \delta\omega_\mu(t)$, where $\Delta\omega_{\mu 0}$ is the static frequency shift caused by the mechanical mode μ at voltage amplitude V_0. The fluctuation $\delta\omega_\mu(t)$ obeys the following differential equation of forced oscillation:

$$\delta\ddot{\omega}_\mu + \frac{2}{\tau_\mu}\delta\dot{\omega}_\mu + \Omega_\mu^2 \delta\omega_\mu = -2k_\mu\Omega_\mu^2 V_0{}^2 \delta v + n(t), \quad (2)$$

where τ_μ, Ω_μ, and k_μ are the decay time, frequency, and coupling constant to the rf field of mechanical mode μ,

---

* kamigait@riken.jp

respectively. The voltage amplitude V is defined as $V = V_0(1 + \delta v)$. The term $n(t)$ is the driving force representing mechanical impacts, which causes microphonics. Therefore, the mechanical vibration can be investigated through the measurement of the instantaneous resonant frequencies.

MEASUREMENT SETUP

Cavity

Figure 1 shows a schematic drawing of the SRILAC cavity, based on the quarter-wavelength resonator (QWR). The design parameters of the cavity are summarized in Table 1. We made ten cavities in total for SRILAC, which are referred to as MRQ-01 – 10, respectively.
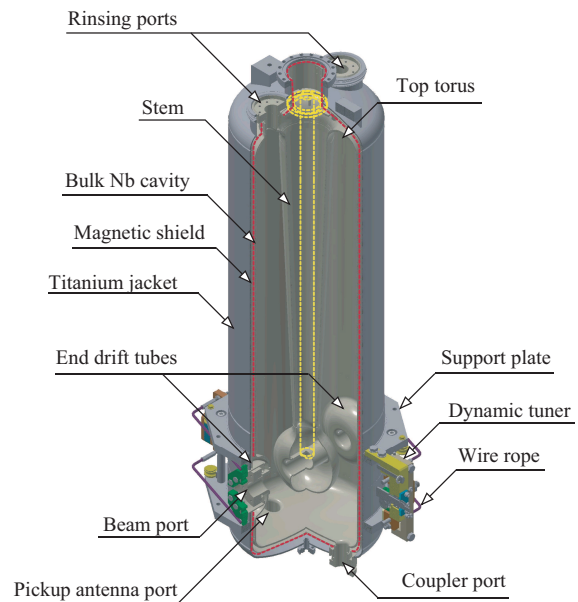

Figure 1: Schematic drawing of the SRILAC cavity [6]. The height of the cavity is 1,103 mm. A magnetic shield is placed between the niobium cavity and the titanium jacket.

Table 1: Design Parameters of the SRILAC Cavity [6].

Parameter	Value
Frequency [MHz] at 4.5 K	73.0
Duty [%]	100 (cw)
β_{opt}	0.08
Height [mm]	1,103
L_{cav} [mm]	320
Total gap voltage [MV] for β_{opt}	2.2
E_{acc} [MV/m] for β_{opt}	6.8
Target Q_0 at 6.8 MV/m	1×10^9
Q_{ext}	$1 - 4.5 \times10^6$

All cavities were made from a bulk niobium sheet of thickness 3.5 – 4 mm with a residual resistance ratio (RRR) of 250. Their inner surfaces are processed by buffered chemical polishing (BCP). Each bulk niobium cavity is contained within a helium jacket made of pure titanium. A magnetic shield is placed between the niobium cavity and the titanium jacket, as shown in Fig. 1. The height and inner diameter of the cavity are 1,103 mm and 300 mm, respectively.

The goal of the unloaded Q-value (Q_0) is set to be 1×10^9 at the designed acceleration voltage E_{acc} of 6.8 MV/m. The rf power coupler is designed so that the external Q-value (Q_{ext}) can be changed from 1×10^6 to 4.5×10^6 by changing the insertion distance. The smallest value of $Q_{ext} = 1 \times 10^6$ was chosen to operate the cavity with a bandwidth of 60 Hz. An rf amplifier of 7.5 kW is prepared for each cavity.

Vertical Test Stand

A vertical test stand was constructed at RIKEN, as shown in Fig. 2 [7]. The inner dimensions of the cryostat are 700 mm in diameter and 3,220 mm in depth. The top torus of the niobium cavity, shown in Fig. 1, is located approximately 1,750 mm below the top flange. A Mu-metal magnetic shield surrounds the interior of the cryostat, and the residual magnetic field in the cryostat was measured to be less than 10 mG.
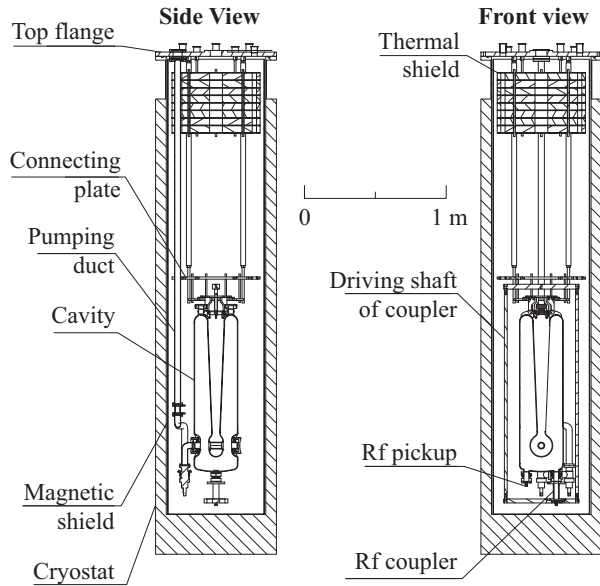

Figure 2: Layout of the test stand with a cavity under vertical test. Bare cavities without the titanium jacket are held at the top torus of the niobium cavity.

As shown in Fig. 2, the bare niobium cavities without the titanium jackets were held at the top torus of the cavity. After the titanium jackets were welded on the niobium structure, the cavities were held at the support plate, which is indicated in Fig. 1, with four long rods suspended from the connection plate. The rf coupler has a long driving shaft that is suspended from the top flange of the cryostat.

Measurement Circuit

The rf circuit used for the vertical test is shown in Fig. 3, which was assembled following Reference [12]. The details of the vertical test have been presented in Reference [8]. An important point is that the rf frequency of the signal generator was always tuned to the instantaneous resonant frequency through feedback control using the phase lock loop between P_{in}, the input signal from the driver amplifier to the cavity, and P_t, the output signal from the cavity. Therefore, the instantaneous frequency is directly measured with the frequency counter in Fig. 3. On the other hand, there is no feedback loop for the voltage in this circuit.
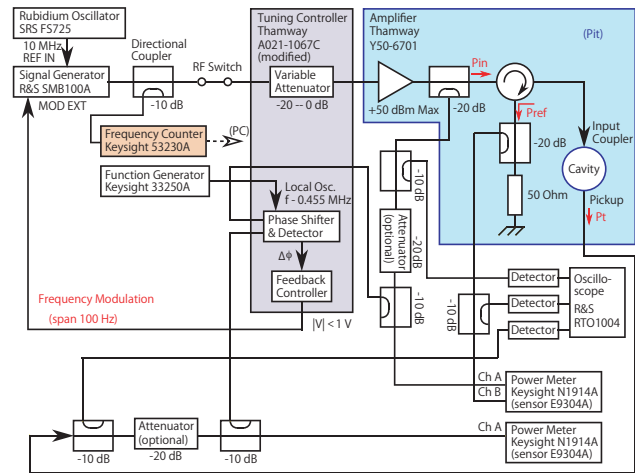

Figure 3: Circuit diagram used in the vertical test of the cavity [8].

Measurements of the frequency shift were carried out during the Q-slope measurements for six bare cavities without titanium jackets (MRQ-05 – 10) and four cavities that were fully assembled with jackets (MRQ-01 – 04) at several acceleration gradients E_{acc}. During each measurement, the loaded Q (Q_L) of the cavity was set to be approximately 7×10^8. The instantaneous frequency was measured with the frequency counter at a time interval of 1 ms during a period of 10 seconds. Each data set containing 10,000 instantaneous resonant frequencies was recorded as a time series. The amplitude of the cavity voltage, which was monitored by a power meter and an oscilloscope, was very stable during each measurement.

DATA ANALYSIS

Frequency Fluctuation

As mentioned above, each time series has $N = 10,000$ data of instantaneous frequencies, $f(n\tau)$, where $n = 1, \cdots, N$ and $\tau (= 1 \text{ [ms]})$ is the time interval of the measurement. For each time series, the fluctuations of the instantaneous frequencies were first calculated as follows:

$$\delta f(n\tau) \equiv f(n\tau) - \frac{1}{N}\sum_{n=1}^{N} f(n\tau). \qquad (3)$$

Facilities - Progress

status report of funded machines

Typical examples of the frequency fluctuation of the cavity are given in Fig. 4. The upper panel represents the fluctuation observed in MRQ-06 without the titanium jacket during the cw operation at E_{acc}= 6.0 [MV/m]. Oscillation of approximately 50 Hz is observed with a fluctuation amplitude of approximately 5 Hz. The fluctuation amplitudes of the bare cavities were of approximately the same order.

The lower panel of Fig. 4 represents the frequency fluctuation in MRQ-03 with the titanium jacket at the same E_{acc} as the top figure. As shown in the figure, the fluctuation amplitude is reduced significantly compared with the data without the jacket.
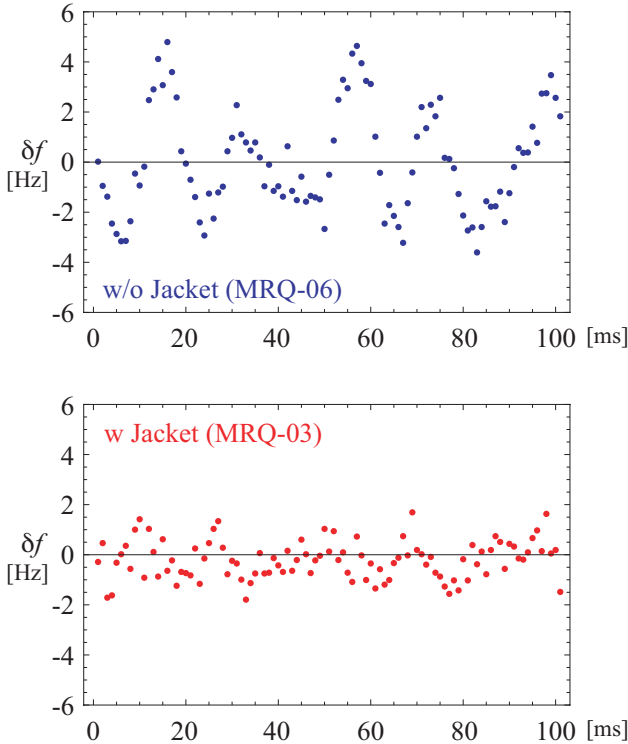

Figure 4: Examples of frequency fluctuation of the cavity. The upper panel represents the fluctuation observed in MRQ-06 without the titanium jacket during the cw operation at E_{acc}= 6.0 [MV/m]. Data of 100 ms were taken from the time series recorded for 10 s. The lower panel represents the fluctuation in MRQ-03 with the titanium jacket welded on the niobium structure. The acceleration gradient E_{acc} was also 6.0 MV/m.

Autocorrelation Function

In order to see the mechanical vibration more clearly, an autocorrelation function was calculated for the time series of $\delta f(n\tau)$, following Reference [11]. The autocorrelation function R_k is defined as follows in the present paper:

$$R_k = \frac{1}{N} \sum_{n=1}^{N-k} x_n x_{n+k}, \qquad (4)$$

where k is the lag of the correlation, and we set $x_n \equiv \delta f(n\tau)$ for simplicity.
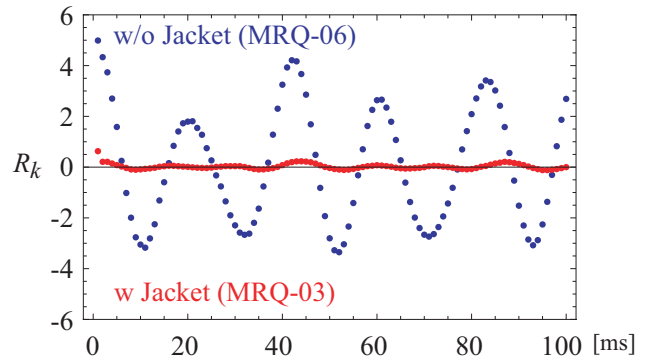

Figure 5: Autocorrelation function calculated for lag up to 100 ms using the time series shown in part in Fig. 4.

Figure 5 shows the correlation function calculated for the two time series of fluctuation shown in part in Fig. 4. The autocorrelation function for MRQ-06 clearly exhibits an oscillation of approximately 50 Hz. Oscillation with a smaller amplitude is now visible in the data of MRQ-03 with the titanium jacket.

Power Spectrum

Using the autocorrelation function calculated above, we estimated the power spectrum of the frequency fluctuation as follows. The autocorrelation R_k was extended to negative values of k by setting

$$R_k \equiv R_{-k}, \qquad (5)$$

and the following definition was adopted for the estimation of the power spectrum in the present study:

$$S(f) = \tau \sum_{k=-(N-1)}^{N-1} R_k \exp\left[-\mathbf{j} \cdot 2\pi f k \tau\right]. \qquad (6)$$

It is easy to show that the above definition is equivalent to the following expression:

$$S(f) = \frac{1}{N\tau} \left| \tau \sum_{n=1}^{N} x_n \exp\left[-\mathbf{j} \cdot 2\pi f n \tau\right] \right|^2. \qquad (7)$$

Figure 6 represents the power spectra calculated with the two time series of fluctuation shown in part in Fig. 4. Many peaks are now visible in the range of mechanical vibration below 100 Hz. As expected, the maximum amplitude of the vibration in the fully assembled cavity of MRQ-03 is smaller by more than 10 dB than that of the bare cavity of MRQ-06. Note, however, that these two power spectra cannot be compared in detail, because they come from different cavities.

DISCUSSIONS

We first compared all of the power spectra of the ten cavities with the mechanical simulations, which was carried out for the bare niobium cavity. According to the simulations, the frequencies of the mechanical vibration of the stem
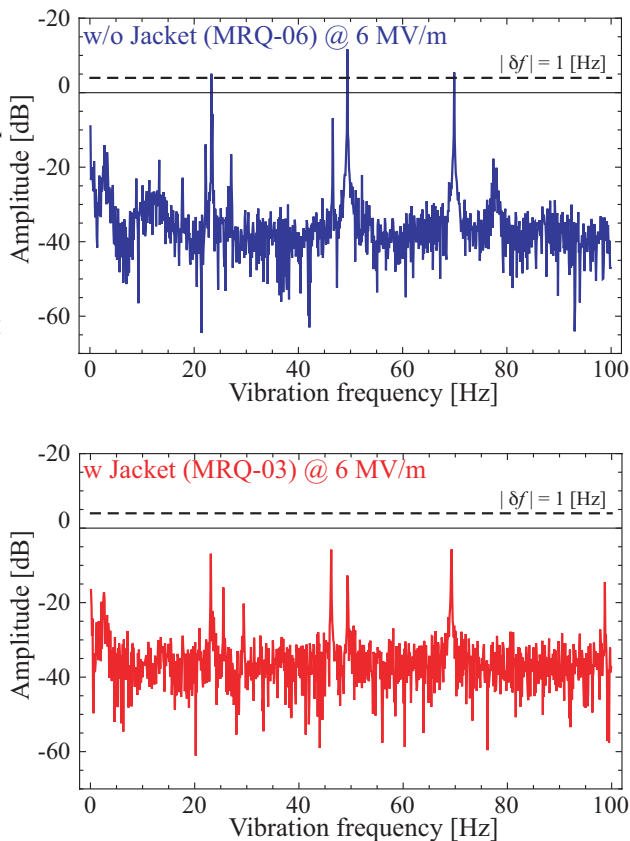
Figure 6: Power spectra calculated with the two data sets shown in part in Fig. 4. The vertical axis shows the amplitude of fluctuation in dB ($10 \log_{10} S(f)$ is plotted). The dashed line in each graph represents a fluctuation amplitude of 1 Hz. Here, δf fluctuates with ± 1 Hz.

Figure 7: Power spectrum of frequency fluctuation measured in MRQ-06 without the jacket at E_{acc}= 4.0 [MV/m] (upper panel) and at E_{acc}= 12.0 [MV/m] (lower panel).

should appear around 40 Hz, whereas the peaks in the measured spectra remain around 50 Hz, as shown in Fig. 6. On the other hand, the simulations do not predict any vibration modes around either 24 Hz or 70 Hz, where strong peaks are observed, as shown in Fig. 6.

In order to investigate the origins of these peaks, we calculated the power spectra at different acceleration gradients E_{acc}. The results are shown in Figs. 7 and 8. As shown in the figures, the amplitudes of the dominant peaks are not strongly dependent on E_{acc}. This means that these peaks do not come from the first term of the right-hand side of Eq. (2), which coincides with the condition $\delta v \approx 0$ observed during the measurements, as mentioned above. In other words, these peaks are microphonics, which are excited by the external impulse.

By considering the mechanical simulations, the peaks around 50 Hz can be attributed to the stem vibrations of the cavity. The other dominant peaks around 24 Hz and 70 Hz might come from the vibrations of the external components in the test stand, which are affected by the environmental conditions. In fact, the peaks around 24 Hz and 70 Hz did not appear in several measurements, which are not shown in the present paper.
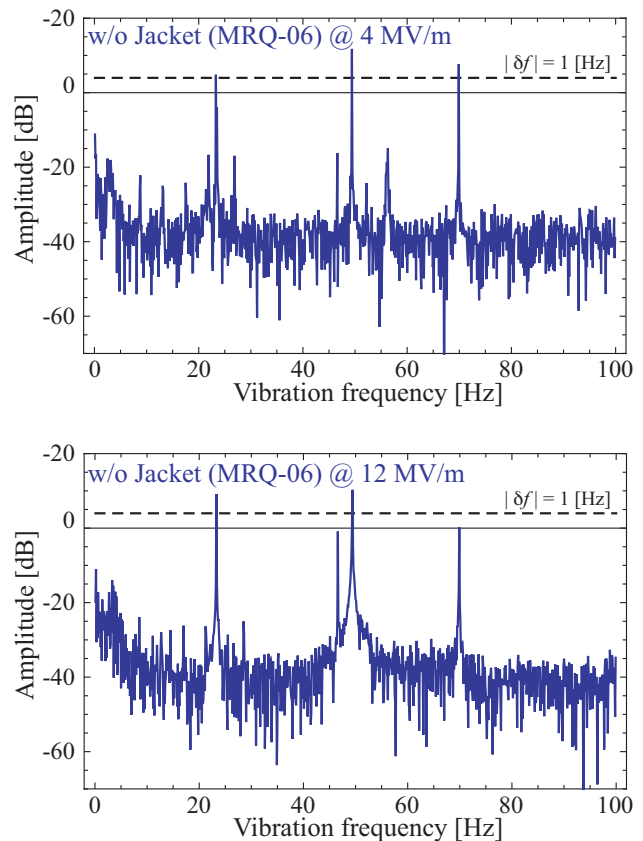
Moreover, we observed that the amplitudes around 50 Hz are smaller in the cavities with titanium jackets. This tendency is also observed in the other cavities, which are not shown in the present paper.

A plausible reason for the change of the amplitude is the difference in mass of the cavities hanging in the test stand. In the lowest-order approximation, the driving term $n(t)$ in Eq. (2) is the inertial force related to the external impact coming through the suspension rods holding the cavity. Since the inertial force is inversely proportional to the mass of the entire cavity, the vibration amplitude is considered to be reduced when the cavity becomes heavier. In SRILAC, the mass is 120 kg for a cavity welded with the jacket, whereas the mass is 55 kg for a bare cavity. Moreover, four stainless steel rods were added to the fully assembled cavity in the test stand. Although this difference could explain the change in the vibration amplitudes, we cannot give definitive evidence, because we did not measure the vibration spectra for the same cavity under the two conditions, i.e., with and without the jacket, under similar environmental conditions. We plan to measure the vibrations in the same way for the cavities in the cryomodules when they are cooled at the RILAC building.
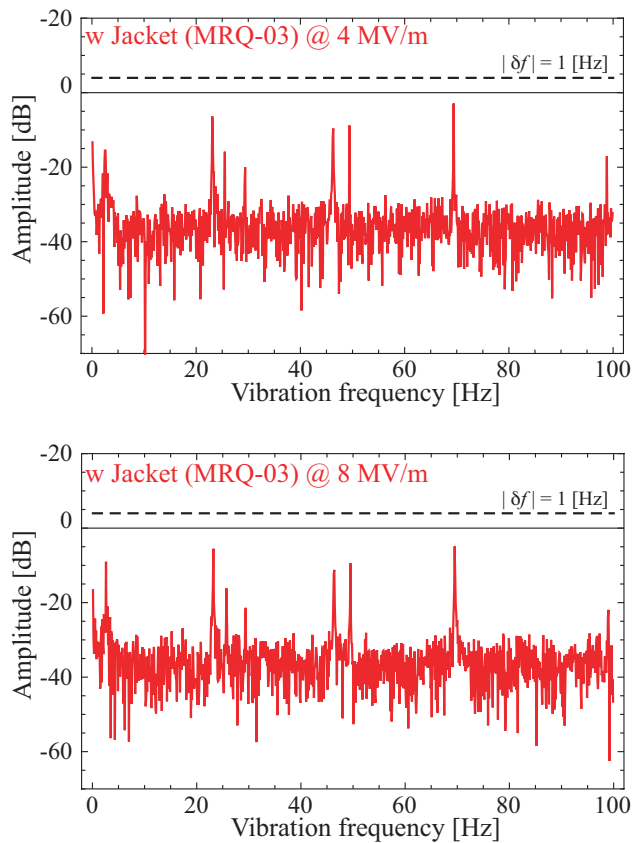
TUP042

516

Figure 8: Power spectra of frequency fluctuation measured in MRQ-03 assembled with the jacket at E_{acc}= 4.0 [MV/m] (upper panel), and at E_{acc}= 8.0 [MV/m] (lower panel).

SUMMARY

We measured the microphonics of the cavities that will be used in SRILAC at RIKEN during a vertical cold test. The mechanical vibration frequencies were extracted from the fluctuations of the resonant frequency through conventional signal analysis. Several peaks appear below 100 Hz. Some of these peaks might have originated from the vibration of the components of the vertical test stand out of the cavities. We also observed that the amplitudes of the fluctuations coming from the stem vibration are smaller in the fully assembled cavities. Measurements of the vibrations will be carried out in the same way when the cavities are cooled in the cryomodules.

ACKNOWLEDGMENTS

REFERENCES

[1] M. Odera *et al.*, "Variable frequency heavy-ion linac, RILAC: I. Design, construction and operation of its accelerating structure", *Nucl. Instr. Meth. Sec. A*, vol. 227, pp. 187–195, 1984. doi:10.1016/0168-9002(84)90121-9

[2] Y. Yano, "The RIKEN RI Beam Factory Project: A status report", *Nucl. Instrum. Methods Sec. B*, vol. 261, pp. 1009–1013, 2007. doi:10.1016/j.nimb.2007.04.174

[3] H. Okuno, N. Fukunishi, O. Kamigaito, "Progress of RIBF accelerators", *Prog. Theor. Exp. Phys.*, vol. 2012, 03C002, 2012. doi:10.1093/ptep/pts046

[4] T. Nagatomo *et al.*, "New 28-GHz Superconducting ECR Ion Source for Synthesizing New Super Heavy Elements of Z > 118", in *Proc. 23th International Workshop on ECR Ion Sources (ECRIS'18)*, Catania, Italy, Sep. 2018, pp. 53–57. doi:10.18429/JACoW-ECRIS2018-TUA3

[5] N. Sakamoto *et al.*, "Development of Superconducting Quarter-Wave Resonators and Cryomodules for Low-Beta Ion Accelerators at RIKEN Radioactive Isotope Beam Factory", presented at the 19th Int. Conf. on RF Superconductivity (SRF'19), Dresden, Germany, Jul. 2019, paper WETEB1, this conference.

[6] N. Sakamoto *et al.*, "Construction Status of the Superconducting Linac at RIKEN RIBF", in *Proc. 29th Linear Accelerator Conf. (LINAC'18)*, Beijing, China, Sep. 2018, pp. 620–625. doi:10.18429/JACoW-LINAC2018-WE2A03

[7] K. Yamada *et al.*, "Construction of Superconducting Linac Booster for Heavy-Ion Linac at RIKEN Nishina Center", presented at the 19th Int. Conf. on RF Superconductivity (SRF'19), Dresden, Germany, Jul. 2019, paper TUP037, this conference.

[8] K. Yamada *et al.*, "First Vertical Test of Superconducting QWR Prototype at RIKEN", in *Proc. LINAC'16*, East Lansing, MI, USA, September 2016, paper THPLR040, pp. 939–942.

[9] J. R. Delayen, "Ponderomotive Instabilities and Microphonics – a Tutorial", *Physica C*, vol. 441, pp. 1–6, 2006.

[10] D. Schulze, "Ponderomotive Stability of R. F. Resonators and Resonator Control Systems", ANL-TRANS-944, Argonne National Lab, 1972.

[11] J. R. Delayen, "Phase and Amplitude Stabilization of Superconducting Resonators", Ph.D. thesis, California Institute of Technology, 1978.

[12] T. Shishido, "Performance evaluation of superconducting cavities", in *Lecture Notes of Accelerator Seminar OHO'14*, Foundation for High Energy Accelerator Science, Tsukuba, Japan, September 2014 (in Japanese).